J. Electrochem. Sci. Eng. **14(2)** (2024) 265-273; http://dx.doi.org/10.5599/jese.2291

Open Access : : ISSN 1847-9286
www.jESE-online.org

Original scientific paper

Additive concentration and nozzle moving speed influence on local copper deposition for electrochemical 3D-printing

Roman Babchuk, Dmytro Uschapovskiy, Victoria Vorobyova, Olga Linucheva, Mykhailo Kotyk and Georgii Vasyliev✉

National Technical University of Ukraine "Igor Sikorsky Kyiv Polytechnic Institute", 37, Prospect Beresteiskyi, Kyiv-56, 03056, Ukraine

Corresponding author: ✉g.vasyliev@kpi.ua; Tel.: +38-096-924-9888; Fax: +38-044-204-9773

Received: February 17, 2024; Accepted: March 21, 2024; Published: March 24, 2024

Abstract

The local deposition process from copper sulfate electrolyte was investigated depending on nozzle moving speed and additive concentration in the electrolyte. A 2×2 cm square model was created and sliced in Ultimaker Cura software, uploaded in a 3D printer, and printed from the copper electrolyte on the stainless-steel surface. Low additive concentration in the electrolyte was found to influence dendrite formation in the corner sections of a square model. Nozzle movement speed was found to influence the deposition area and the thickness of the metal. The lowest tested nozzle movement speed of 5 s / voxel increased the deposition area by nearly 40 % in horizontal direction compared to 2.5 s / voxel. Further increase of nozzle movement speed to 1.6 s / voxel does not change the deposition area. The thickness in the corners increases by 2.5 times compared to the straight section of the square when the nozzle movement speed increases from 5 to 1.6 s / voxel. The non-uniform thickness of the deposited metal is caused by a considerable reduction of nozzle movement speed when it moves through the corner. The results obtained in this work can be further used to develop electrochemical 3D printing technology.

Keywords

Additive manufacturing; copper electroplating; slicing; profilometry

Introduction

Additive manufacturing is a novel and fast-developing technique based on the bottom-up approach. Unlike traditional manufacturing, the part is produced by forming it from the material layer by layer when excessive material is mechanically or physically removed. Non-metallic additive manufacturing technologies are rapidly developing and, in some industries, have already replaced traditional ones, but metal parts additive manufacturing remains a challenge [1,2].

Most metal additive manufacturing technologies require high energy to melt the metal. Laser or electromagnetic sources are used [3,4]. Compared to them, the electrochemical additive manufacturing technique, when metal parts are formed by metal deposition from ions in the electrolyte solution is much cheaper because it does not require high energies and prior preparation of expandable materials.

Different techniques have been developed for electrochemical additive manufacturing (ECAM). They can be divided into two main groups: mask-based and maskless electrochemical manufacturing [5]. It is generally agreed that maskless manufacturing is a more promising technique because it does not require mask preparation and can be performed easily using only electrolyte and electrodes.

Several maskless ECAM techniques with different manufacturing speeds and accuracy are developing. Among them are fluidic force microscope (FluidFM) [6-10], meniscus-confined deposition [11-16], jet electrodeposition [17-19] and localized electrochemical deposition [20-24]. In the localized electrochemical deposition technique, the electric field distribution in the electrolyte determines the deposition area; the electrolyte composition and current mode determine the deposition rate. In our previous works, it was established that electrolyte composition can influence the slope of the polarization curve and influence the deposition area [24].

The aim of the present work is to study the influence of additive concentration in the electrolyte and the 3D-printer nozzle moving speed on the deposition area and thickness distribution of the deposited copper layer.

Experimental

The local electrochemical deposition process was investigated in square model printing. The appearance of the model in the UltiMaker Cura software is shown in Figure 1. The size of the object was 20×20 mm and the height was 2 mm. The object was sliced in g-code with the following parameters: nozzle moving speed F1200, coordinate movement direction (X60.178, Y60.179), layer height (Z0.001) that corresponds to 1 μm in the slicer. The g-code was loaded in a 3D printer.

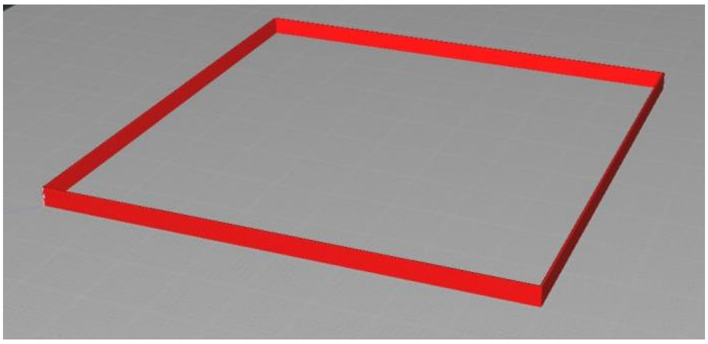

Figure 1. *The appearance of square model, used in 3D printing in the UltiMaker Cura software*

The laboratory setup is shown in Figure 2. The printing process is performed on the surface of the stainless-steel plate placed on the bottom of the plastic vessel. 1 L of electrolyte was poured into the vessel, and its level was 1.5-2 cm above the plate. The vessel was placed inside the 3D printer frame. The steel plate was attached to the negative pole of the direct current source, while the positive pole was attached to the anode placed inside the printer nozzle. The anode was made of lead. An insoluble lead anode was used because lead in a sulfate solution is chemically stable and is potentially cheaper than platinum. The main purpose of the insoluble anode application is to avoid the formation of monovalent copper ions in the solution, which can provoke the formation of coarse crystalline sediments (disproportionation with the formation of metallic dispersed copper, which is transferred to the cathode and provokes the formation of dendrites). The printing process was started by turning on the current once the anode was placed in a certain position of vessel. The current source maintained a constant current value, varying the applied voltage.

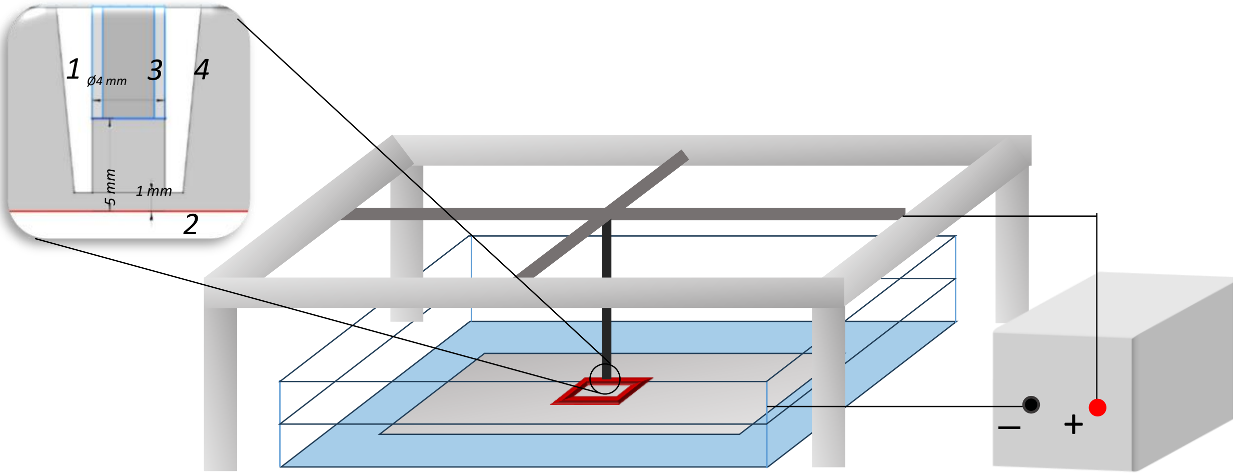

Figure 2. *The laboratory setup for local electrodeposition*

The copper plating electrolyte was used for metallic copper deposition. Two electrolyte compositions were used with different concentrations of the additive. Electrolyte compositions are given in Table 1, while deposition conditions are presented in Table 2. A total of 5 objects were printed in both electrolytes and at 3 different nozzle moving speeds.

Table 1. *Electrolytes composition*

Component	Content, g/L	
	Electrolyte 1	Electrolyte 2
$CuSO_4\cdot 5H_2O$	200	200
H_2SO_4	75	75
KCl	0.3	0.3
Additive RUBIN T-200*	1 mL/L of Rubin T200-A 4 mL/L of Rubin T200-G 1 mL/L of Rubin T200-E	2 mL/L of Rubin T200-A 8 mL/L of Rubin T200-G 2 mL/L of Rubin T200-E

*Leveling and brightness additive, KIESOW OBERFLÄCHENCHEMIE GmbH & Co. KG

Table 2. *Deposition conditions used for local copper deposition investigation*

Exp. No	Electrolyte	Anode moving speed, s/voxel	Applied current density, A / cm^2	Deposition duration, h
1	1	2.5	4	6
2	1	1.6	4	6
3	2	5.0	4	6
4	2	2.5	4	6
5	2	1.6	4	6

The 3D-printed objects were characterized by 3D profilometry. Two cross-sections were measured and used for analysis: a cross-section of the edge and a cross-section of the corner (Figure 3).

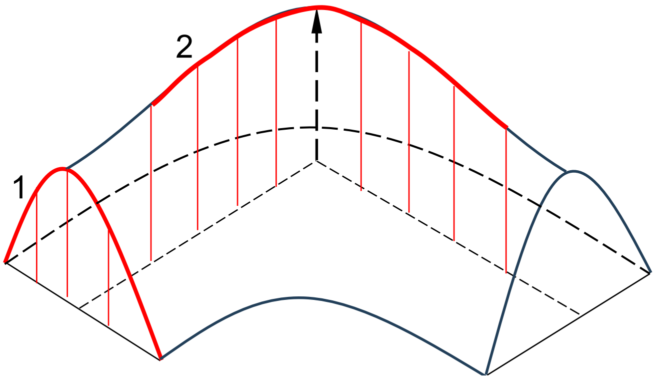

Figure 3. *The scheme showing cross-section regions in the printed square object used for analysis: 1 - cross-section of the edge; 2 - cross-section of the corner*

Results and discussion

The copper deposition process in the sulfate electrolyte is a simple electrochemical process that can be summarized with the equation:

$$Cu^{2+} + 2e^{-} = Cu \tag{1}$$

Every 2 electrons reduce one copper atom, which is deposited on the surface of the metal substrate. According to Faraday's law, the amount of electricity determines the mass of deposited metal. At the same time, the morphology of deposited metal depends on the kinetic parameters of the electrochemical process as well as the electric field distribution between the anode located in the nozzle and a cathode placed at the bottom of the vessel.

The photos of deposited objects are given in Figure 4. All the deposited objects are square-shaped. However, depending on the deposition conditions, the morphology of deposited metal is different.

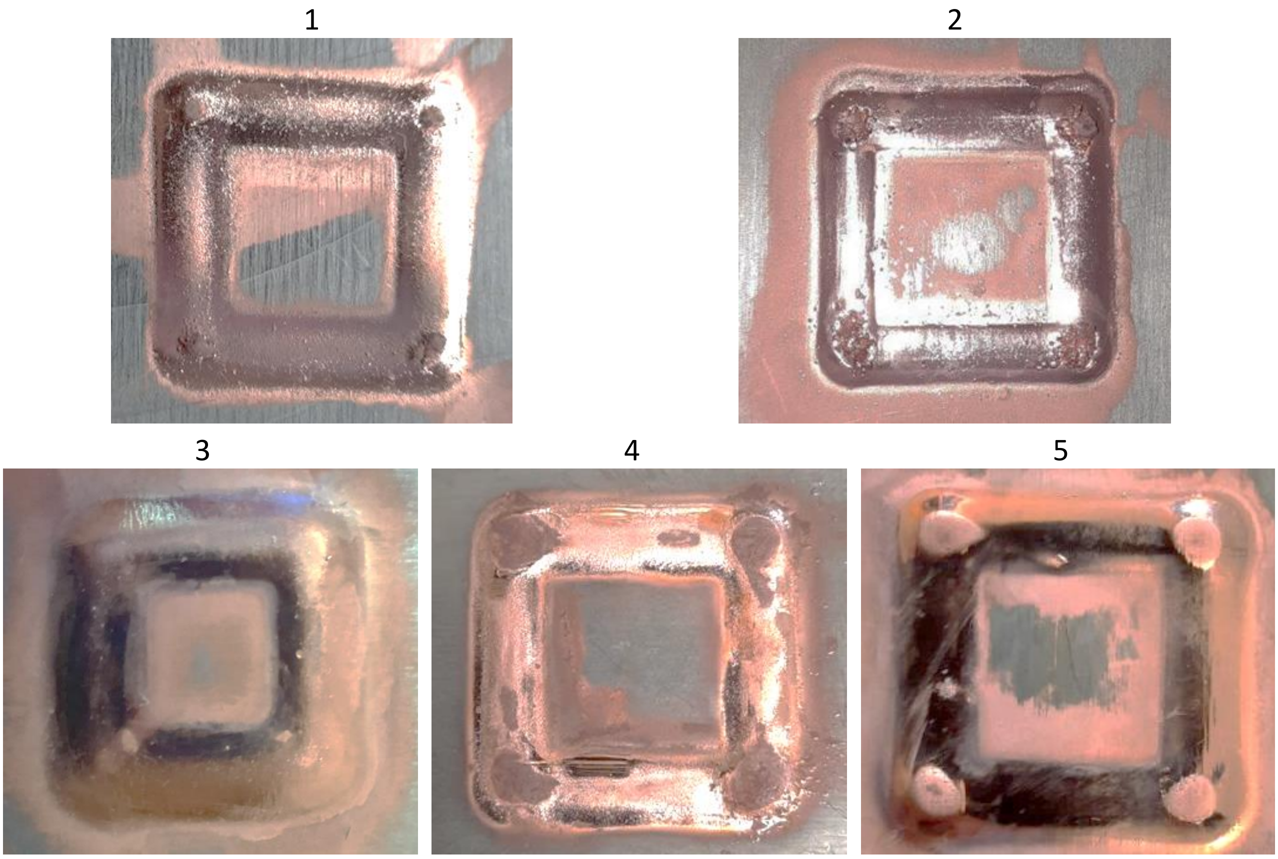

Figure 4. *Photographs of 3D-printed square objects: 1 to 5 - correspond to experiment numbers in Table 2*

In Electrolyte 1, with reduced additive content, the dendrites formation appears in the corners of the square (Figure 4.1, 4.2). Also, the reduction of nozzle moving speed leads to an increase in deposition area (Figure 4.3).

Depending on deposition conditions, size distribution in printed objects was measured using 3D profilometry. The profilograms are shown in Figure 5. The formation of dendrites is clearly visible in the corner section for the objects printed in Electrolyte 1 at both nozzle moving speeds. The cross-sections of printed objects are presented in Figures 6 and 7.

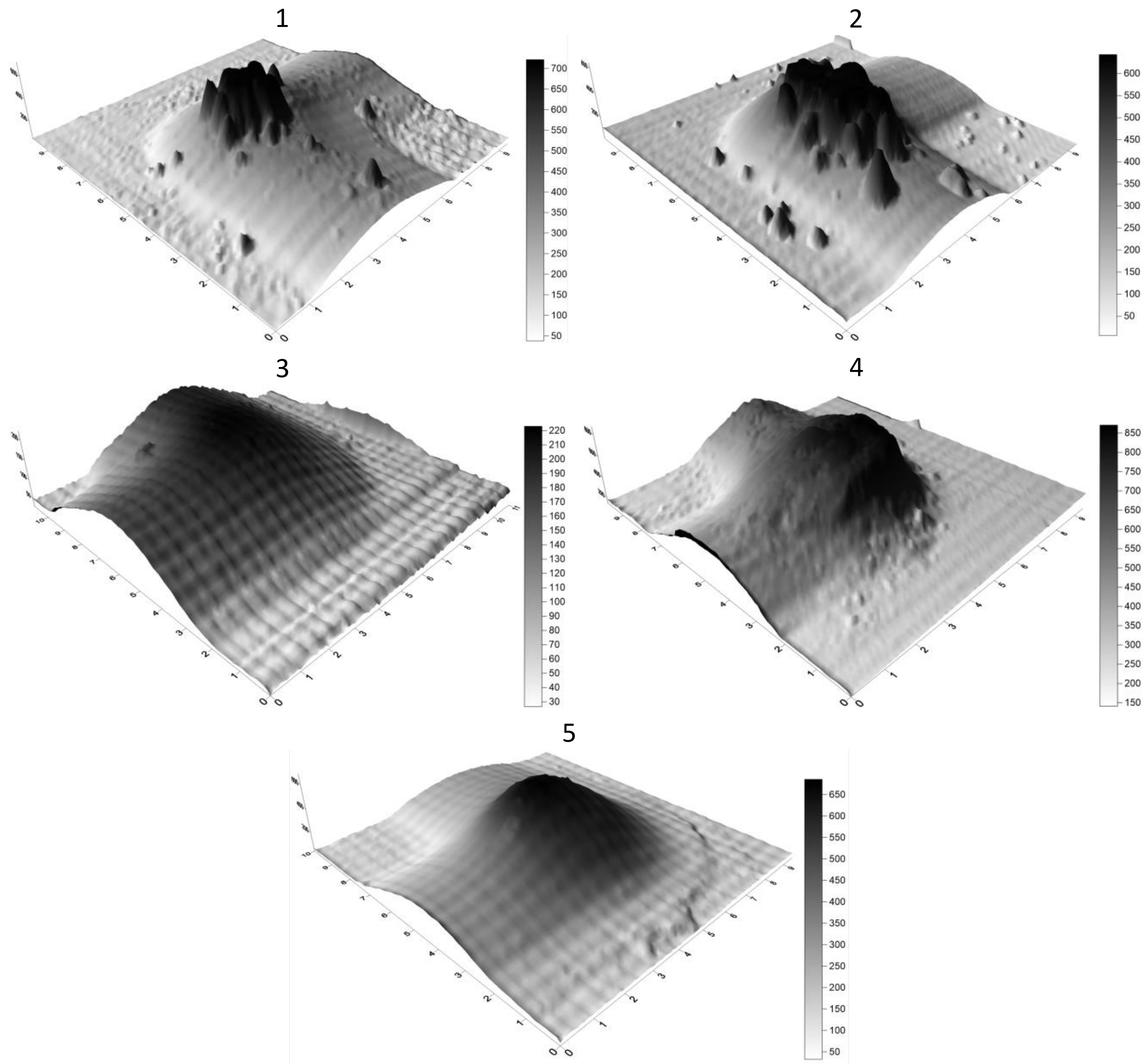

Figure 5. *Profilograms of 3D-printed square objects: 1 to 5 - correspond to experiment numbers in Table 2*

Figure 5 (1,2) shows active dendrite formation on the corner section of the square. The cross-section profile (Figure 7, curve 1, 2) shows that the height of dendrites is nearly the height of the deposited metal thickness. The reason for dendrite formation is the high current density in the corner section and a longer period of deposition because the anode stays longer above the corner compared to the straight section of the square edge. An increase in the thickness of the copper deposit, as well as the formation of dendrites at the corners, is associated with a decrease in the speed of movement and some delay of the nozzle when passing the corner of the trajectory. As a result, the amount of electricity that falls on this part of the trajectory increases, and because of slowing down, the average current density will increase, which provokes dendrite formation. The dendrite formation problem is solved by increasing the additive concentration. The additive is known to increase the deposition polarization, thus reducing the deposition rate. In this work, the dendrite formation was hindered when additive concentration was corrected according to recommendation: 2 mL/L of Rubin T200-A, 8 mL/L of Rubin T200-G and 2 mL/L of Rubin T200-E.

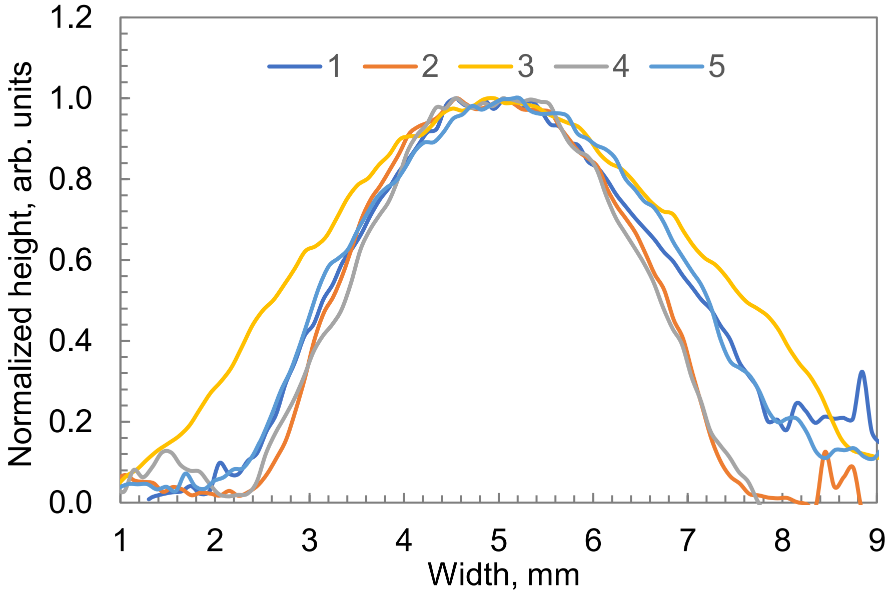

Figure 6. *Typical cross-section of the edge of the printed square object. Numbers 1 to 5 correspond to experiment numbers in Table 2*

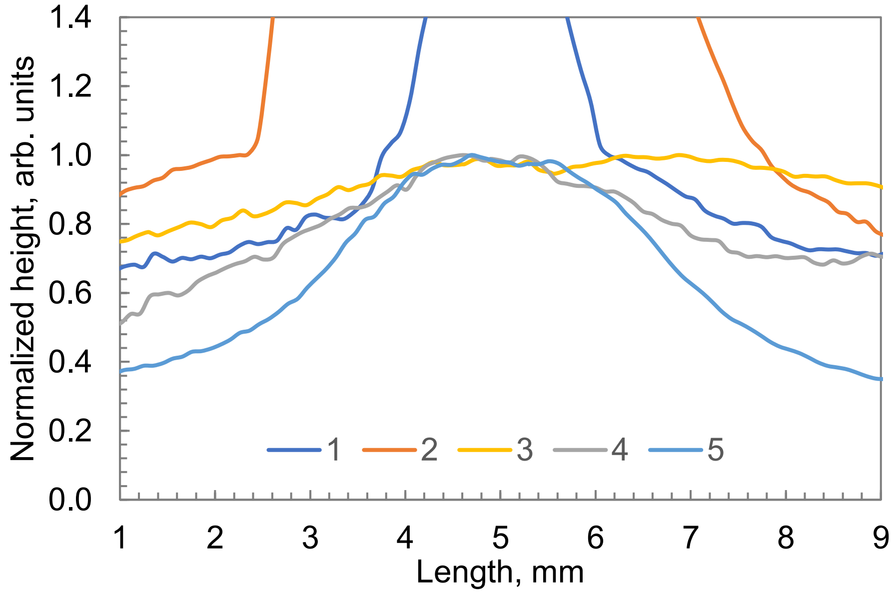

Figure 7. *Typical cross-section of the corner of the printed square object. Numbers 1 to 5 correspond to the experiment number in Table 2*

The movement speed of the nozzle influences the deposition process in both the corner and straight sections. Very low speed increased the deposited metal area. The cross-section of the edge shows a 40 % wider deposition area. The increase in nozzle movement speed from 2.5 to 1.6 s/voxel does not further reduce the deposited surface area.

In the corner section, the lowest tested speed of 5 s/voxel, the most uniform layer was deposited. The thickness of the deposited metal in the corner is only 15 % higher than on the edge. The next tested speed of 2.5 s/voxel increased the thickness in the corner to 1.5 times, and when the nozzle speed reached 1.6 s/voxel, the corner thickness was nearly 2.5 times higher than the edge one.

The change in the deposited metal thickness in the corner section is caused by the reduction of nozzle movement speed (Figure 8). At the lowest tested speed of 5 s/voxel, the nozzle moves through the corner section with nearly the same speed as through the straight section. Thus, the amount of deposited metal remains the same. When the speed increases to 2.5-1.6 s/voxel, the nozzle passes the straight section faster than the corner section. So, the thickness of the deposited metal on the straight section becomes lower, and in the corner section – higher.

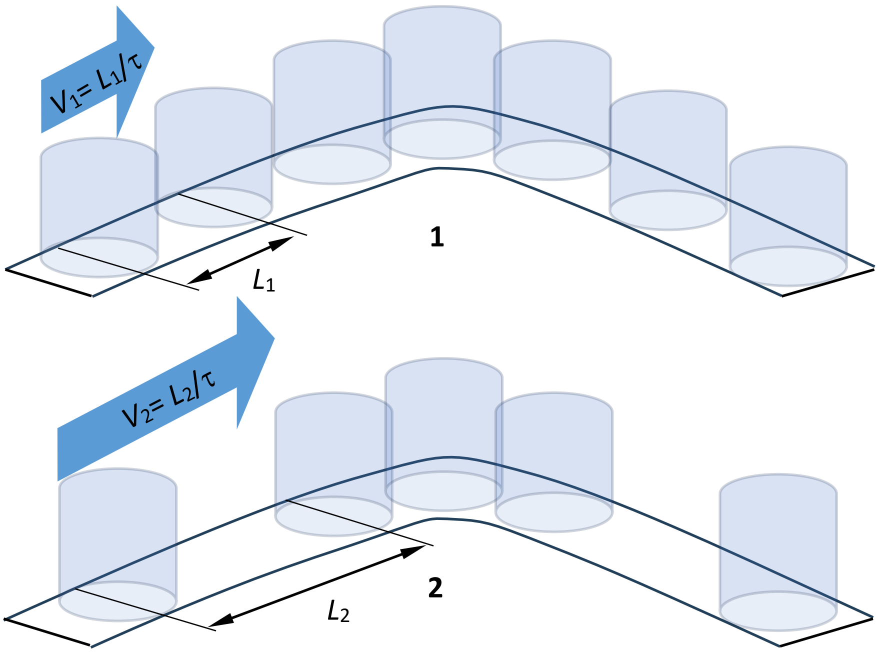

Figure 8. *Schematic explanation of nozzle moving speed influence on the thickness of deposited metal: 1 - low nozzle moving speed; 2 - high nozzle moving speed*

Further investigation should be aimed at current control over the corners in a manner that reduces the current value proportional to the speed reduction.

Conclusions

The local deposition process from copper sulfate electrolyte was investigated. The additive concentration in the electrolyte was found to influence dendrite formation. The dendrites are formed on the corner sections of a square model. The use of recommended additive concentration 2 mL/L of Rubin T200-A, 8 mL/L of Rubin T200-G and 2 mL/L of Rubin T200-E reduces the formation of dendrites.

Nozzle movement speed influences the deposition area of the metal and its thickness. The lowest tested nozzle movement speed of 5 s / voxel increased the deposition area by nearly 40 % compared to 2.5 s/voxel. Further increase of nozzle movement speed to 1.6 s/voxel does not change the deposition area.

The increase in nozzle movement speed influences the deposited metal thickness in the corner sections. The thickness in the corners increases by 2.5 times compared to the edges of the square when the nozzle movement speed increases from 5 to 1.6 s/voxel.

The results obtained in this work can be further used to develop electrochemical 3D printing technology. The further investigation direction should be aimed at current control over the corners in a manner that reduces the current value proportional to the speed reduction.

***Acknowledgements**: This work was supported by the Ministry of education and science of Ukraine (Reg. number 0122U001523, 2022).*

References

[1] I. Gibson, D. Rosen, B. Stucker, *Additive Manufacturing Technologies*, Springer, New York, USA, 2010, p. 472. https://doi.org/10.1007/978-1-4419-1120-9

[2] A. Serajuddin, Challenges, current status and emerging strategies in the development of rapidly dissolving FDM 3D-printed tablets: An overview and commentary, *ADMET and DMPK* **11** (2023) 33-55. https://doi.org/10.5599/admet.1622

[3] W. E. Frazier, Metal additive manufacturing: a review, *Journal of Materials Engineering and Performance* **23** (2014) 1917-1928. https://doi.org/10.1007/s11665-014-0958-z

[4] D. Herzog, V. Seyda, E. Wycisk, C. Emmelmann, Additive manufacturing of metals, *Acta Materialia* **117** (2016) 371-392. https://doi.org/10.1016/j.actamat.2016.07.019

[5] X. Li, P. Ming, S. Ao, W. Wang, Review of additive electrochemical micro-manufacturing technology, *International Journal of Machine Tools and Manufacture* **173** (2022) 103848. https://doi.org/10.1016/j.ijmachtools.2021.103848

[6] G. Ercolano, T. Zambelli, C. van Nisselroy, D. Momotenko, J. Vörös, T. Merle, W.W. Koelmans Multiscale additive manufacturing of metal microstructures, *Advanced Engineering Materials* **22** (2020) 1900961. https://doi.org/10.1002/adem.201900961

[7] L. Hirt, R.R. Grüter, T. Berthelot, R. Cornut, J. Vörös, T. Zambelli, Local surface modification via confined electrochemical deposition with FluidFM, *RSC Advances* **103** (2015) 84517-84522. https://doi.org/10.1039/c5ra07239e

[8] W. Ren, J. Xu, Z. Lian, P. Yu, H. Yu, Modeling and experimental study of the localized electrochemical micro additive manufacturing technology based on the fluidFM. *Materials* **13** (2020) 2783. https://doi.org/10.3390/ma13122783

[9] G. Ercolano, C. van Nisselroy, T. Merle, J. Vörös, D. Momotenko, W. W. Koelmans, T. Zambelli Additive manufacturing of sub-micron to sub-mm metal structures with hollow AFM cantilevers, *Micromachines* **11** (2020) 6. https://doi.org/10.3390/mi11010006

[10] W. Ren, J. Xu, Z. Lian, X. Sun, Z. Xu, H. Yu, Localized electrodeposition micro additive manufacturing of pure copper microstructures, *International Journal of Extreme Manufacturing* **4** (2021) 015101. https://doi.org/10.1088/2631-7990/ac3963

[11] A. Ambrosi, R. D. Webster, M. Pumera, Electrochemically driven multi-material 3D-printing. *Applied Materials Today* **18** (2020) 100530. https://doi.org/10.1016/j.apmt.2019.100530

[12] S. Burlison, M. Minary-Jolandan, Multiphysics simulation of microscale copper printing by confined electrodeposition using a nozzle array, *Journal of Applied Physics* **131** (2022) 055303. https://doi.org/10.1063/5.0072183

[13] Y. Guo, P. Liu, P. Jiang, Y. Hua, K. Shi, H. Zheng, Y. Yang, A flow-rate-controlled double-nozzles approach for electrochemical additive manufacturing. *Virtual and Physical Prototyping* **17** (2022) 52-68. https://doi.org/10.1080/17452759.2021.1989751

[14] X. Chen, X. Liu, P. Childs, N. Brandon, B. Wu, A low cost desktop electrochemical metal 3D printer, *Advanced Materials Technologies* **10** (2017) 1700148. https://doi.org/10.1002/admt.201700148

[15] F. Zhang, D. Li, W. Rong, L. Yang, Y. Zhang, Study of microscale meniscus confined electrodeposition based on COMSOL, *Micromachines* **12** (2021) 1591. https://doi.org/10.3390/mi12121591

[16] X. Chen, X. Liu, M. Ouyang, J. Chen, O. Taiwo, Y. Xia, P. Childs, N.P. Brandon, B. Wu, Multi-metal 4D printing with a desktop electrochemical 3D printer, *Scientific Reports* **9** (2019) 3973. https://doi.org/10.1038/s41598-019-40774-5

[17] S.J. Dover, A.E.W. Rennie, G.R. Bennett, Rapid Prototyping Using Electrodeposition of Copper, *Solid Freeform Fabric Symposium*, 1996, pp. 191-198. http://hdl.handle.net/2152/69936

[18] H. Fan, Y.P. Zhao, S.K. Wang, Technical study of Jet electrodeposition in manufacture of metal parts, *Key Engineering Materials* **667** (2016) 259-264. https://doi.org/10.4028/www.scientific.net/KEM.667.259

[19] C. Wang, L.D. Shen, M.B. Qiu, Z.J. Tian, W. Jiang, Characterizations of Ni-CeO_2 nanocomposite coating by interlaced jet electrodeposition, *Journal of Alloys and Compounds* **727** (2017) 269-277. https://doi.org/10.1016/j.jallcom.2017.08.105

[20] E. M. El-Giar, R. A. Said, G. E. Bridges, D. J. Thomson, Localized electrochemical deposition of copper microstructures, *Journal of The Electrochemical Society* **147** (2000) 586-591. https://doi.org/10.1149/1.1393237

[21] C. Y. Lee, C. S. Lin, B. R. Lin, Localized electrochemical deposition process improvement by using different anodes and deposition directions, *Journal of Micromechanics and Microengineering* **18** (2008) 105008. https://doi.org/10.1088/0960-1317/18/10/105008

[22] J. C. Lin, T. K. Chang, J. H. Yang, Y. S. Chen, C. L. Chuang, Localized electrochemical deposition of micrometer copper columns by pulse plating, *Electrochimica Acta* **55** (2010) 1888-1894. https://doi.org/10.1016/j.electacta.2009.11.002

[23] G. Vasyliev, V. Vorobyova, D. Uschapovskiy, O. Linyucheva, Local electrochemical deposition of copper from sulfate solution, *Journal of Electrochemical Science and Engineering* **12** (2022) 557-563. http://dx.doi.org/10.5599/jese.1352

[24] G. Vasyliev, V. Vorobyova, D. Uschapovskiy, O. Linyucheva, Influence of polarization curve slope on the accuracy of local copper electrodeposition from sulphate electrolyte, *Journal of Electrochemical Science and Engineering* **6** (2023) 971-980. https://doi.org/10.5599/jese.1899